Available at: http://www.ictp.trieste.it/~pub_off IC/2004/1

United Nations Educational Scientific and Cultural Organization
and
International Atomic Energy Agency

THE ABDUS SALAM INTERNATIONAL CENTRE FOR THEORETICAL PHYSICS

CORRELATION BETWEEN LOCAL SLIP RATE AND LOCAL HIGH-FREQUENCY RADIATION CAPABILITY IN AN EARTHQUAKE FAULT

A.A. Gusev
Institute of Volcanic Geology and Geochemistry, Russian Academy of Science,
9 Piip Blvd., Petropavlovsk-Kamchatsky, 683006, Russian Federation
and
Kamchatkan EM Seismological Department, GS RAS,
9 Piip Blvd., Petropavlovsk-Kamchatsky, 683006, Russian Federation,

E.M. Guseva and V.M. Pavlov
Kamchatkan EM Seismological Department, GS RAS,
9 Piip Blvd., Petropavlovsk-Kamchatsky, 683006, Russian Federation

and

G.F. Panza
Department of Earth Sciences, University of Trieste,Via E. Weiss 4, 34127 Trieste, Italy
and
The Abdus Salam International Centre for Theoretical Physics, SAND Group, Trieste, Italy.

MIRAMARE - TRIESTE

January 2004

Abstract

For any earthquake, the slipping fault area and the source of high-frequency seismic waves, by and large, coincide. However on a more local scale the areas of high seismic slip rate and of increased high-frequency radiation capability (increased HF seismic luminosity) need not to be closely correlated. To study in more detail how slip rate and seismic luminosity are interrelated, a systematic analysis is performed that uses teleseismic P-waves of 23 intermediate-depth earthquakes of magnitude above 6.8. From each of the 344 "raw" broadband time functions, we first determine two time histories: (1) displacement and (2) squared, 0.5-2.5Hz band-passed, velocity, or "power", and then calculate the correlation coefficient, ρ, between them. The 0.5-2.5 Hz "power" signal is distorted by the scattering in the Earth that smears it and generates P-coda. To overcome this difficulty, before performing the correlation analysis, the displacement is artificially distorted through the convolution with an appropriate time function, that simulates the scattering in the Earth. Even if a perfect correlation between fault slip and seismic luminosity is assumed the estimated values of ρ will be somewhat lower than unity, because of the random character of high-frequency waves. We estimated the average value ρ=0.52 for the correlation coefficient between the radiated time histories for displacement and "power". This value can be ascribed to the similar correlation coefficient between slip rate and HF seismic luminosity over the source area. When two contributing factors - fluctuations and genuine mismatch of slip rate and mean luminosity - are isolated, fluctuations produce ρ=0.72 and the mismatch produces ρ=0.83. Thus the observed values of ρ indicate genuine differences between the distributions of the slip rate and the seismic luminosity over the fault area. These results provide important constraints both for the accurate wide-band simulation of strong ground motion and for theoretical dynamic source models.

INTRODUCTION

In modern seismology, it is widely accepted that the source of seismic waves, including high-frequency (HF) waves, is a fast-slipping patch on a geological fault, named earthquake fault. This means: no slip, no HF seismic energy; and, neglecting creeping faults or fault patches, this is generally true. However, the majority of fault models that deal with high-frequency radiation assume more than that. The common property of the fault models, usually implicit, is that the HF radiation increases with increasing slip rate, or, for composite models, that HF energy increases with increased subsource seismic moment. Examples are the composite models formulated by Blandford (1974), Hanks (1979), Boatwright(1982; 1987), Papageorgiou and Aki (1983), and Gusev(1989). This property of the listed models can be considered a reasonable initial approximation. To find out how close, in real earthquakes, it is the actual correlation between slip rate and HF radiation capability an independent inversion for each of the two quantities is needed. For brevity, from now on, we shall call the HF radiation capability, or more accurately the radiated power per unit source area, "seismic luminosity", transferring to seismology the standard light-engineering term for the similar parameter used to specify the radiated light power. In seismology, we additionally need a term for the (total) radiated HF *energy* per unit source area, that is for the integral of seismic luminosity over the source duration time, or essentially over the rise time; we can call this integral "cumulative seismic luminosity". We shall not mention common luminosity any more, and for brevity we will use the term "luminosity" meaning "seismic luminosity". Distributions of luminosity peak values and of cumulative luminosity over the fault area are probably strongly correlated, because the value of the rise time does not seem to vary too much over the fault area, as it follows from (Heaton 1990).

At present, a considerable number of inversions for space-time distributions of luminosity or cumulative luminosity have been performed (Iida & Hakuno, 1984; Gusev and Pavlov, 1992, 1997; Zeng et al., 1993; Kakehi and Irikura, 1995; Nishimura et al., 1996). These inversions show that the spatial distributions of luminosity (or cumulative luminosity) generally resemble those of the slip rate, but do not coincide with them and sometimes significant differences can be seen. Therefore observational data generally do not strongly support the idea that luminosity is tightly related to the slip rate.

The inversion of the slip rate and luminosity distributions in space-time is a complicated and error-prone procedure with limited resolution. In the following we try to derive information on slip-luminosity correlation directly from far-field (teleseismic) body-wave records, which clearly bear some information on this unknown. A potential difficulty of this approach is the fact that the formation of a far-field body wave pulse is a kind of projection from 3D to 1D, with possible loss of information. However, this seems to be only an apparent problem. It will be shown that, at least in the simplest approximation of a completely incoherent source, one can merely equate the level of correlation between far-field displacement time history and far-field HF squared velocity or "power" time history on one side, and a similar level for source slip rate and source luminosity, on the other side. Therefore, from an analysis of body wave data one can directly deduce properties of fault radiation.

To obtain an estimate of such an empirical kind is interesting, and also rather valuable from the practical viewpoint, because it can be used to verify and/or improve wideband models of fault radiation used for the prediction of strong ground motion. However, from a more general viewpoint it is far from being satisfactory. As well known, after band-pass filtering by an octave or comparable filter, the HF body wave signal from an earthquake looks much like a non-stationary random signal, or modulated noise. It is natural, and was proposed long ago, to treat such a signal as a realization (sample function) of a random process. Departing from the notion of random process we can introduce, for a given frequency band, a mean, "ideal" time history of power (ensemble mean, or modulating function, or mean envelope). This mean power signal is a kind of ideal object, unobservable directly. Generally speaking, it might be estimated from data very accurately with sufficiently wide-band data. Unfortunately, seismological data are narrow-band and the difference between "ideal" and observed power signal must be substantial. This difference often labeled as "the effect of random fluctuations".

Consider now the reference case, when the source mean power signal at HF is accurately proportional to the slip rate, or the body wave mean power signal is proportional to wave displacement. With "ideal" signals, the correlation coefficient will be equal to unity. With real signals, random fluctuations will bring this coefficient down. (To what extent, depends on the bandwidth). It is important to distinguish between this "fluctuational" decorrelation, rooted in physically uninteresting inherent fluctuations of random signal, and the "physical" decorrelation related to the lack of mentioned proportionality (and giving us some important information regarding the source process). Let us now represent these ideas in parametric form.

When both kinds of decorrelation operate, we must distinguish between three kinds of correlation coefficient: (1) observed one, i.e. between observed displacement and observed squared filtered velocity, denoted ρ_{ob}, (2) "ideal" one, between observed displacement and (unobservable) mean power, denoted ρ_{id} and (3) reference one: the mean value of ρ_{ob} for the hypothetic case when only "fluctuational" decorrelation is present (and the correlation between observed displacement and "mean" power is perfect); we denote it ρ_{obmax}. This last value gives us the maximum among average observed correlation values obtained with different possible values of ρ_{id} . We shall estimate this value through Monte-Carlo simulation.. There is no real interest to show that ρ_{ob} is significantly below unity because this is the trivial outcome of "fluctuational" decorrelation. What deserves efforts is to show that ρ_{ob} is significantly lower than ρ_{obmax}, or equivalently that ρ_{id} is less than unity. This is the aim of the present study. Note that the entire above discussion of mean and observed body wave signals is equally applicable to the time history of an earthquake source.

When one tries to analyze correlation between displacement and HF power signals, one meets with a problem: the HF signal is markedly distorted by scattering along the path (this is evident as the formation of P coda). To bypass this obstacle, before comparing displacement and "power" signal, we artificially distort the displacement signal by convolution with an analog of the "power Green's function of the medium".

The plan of the work is as follows. (1) To provide a general background to our data analysis we introduce the general notion of seismic luminosity, and discuss the difference between the "ideal" case, when random fluctuations are absent, and the case of real observations. We also analyze a few other theoretical points important for data processing and interpretation. (2) We decide to use teleseismic P waves from large intermediate-depth earthquakes, thus providing sufficiently long wide-band records of relatively "clean" body waves, and we select the particular frequency band to determine HF power signal. (3) We select records with good S/N ratio and with clear one-sided displacement signal. (4) We select an appropriate envelope function that emulates the formation of P-coda and we distort displacement signals using this envelope. (5) We calculate empirical correlation coefficients between displacement and HF squared power. (6) We determine the expected value for the same correlation coefficient for the ideal case when decorrelation is caused only by random fluctuations of the HF signal. We find that the empirical correlation is lower than the one expected purely from fluctuations, and we show that this difference is statistically significant. (7) We estimate the level of correlation between source slip rate and *mean* source luminosity, that is, for the ideal case with fluctuations completely suppressed.

THEOREICAL BACKGROUND FOR DATA ANALYSIS

Introducing luminosity

Let us consider an infinite elastic space with Lame's constant λ and μ and density ρ, that contains a planar shear fault that occupies the finite area Σ on a plane with unit normal $\boldsymbol{n}$. Let $\boldsymbol{x}=\{x_k\}=\{x_1, x_2, 0\}$ be the coordinates on the fault plane, with their origin at the hypocenter, and let $\boldsymbol{\xi}=\{\xi_1, \xi_2, \xi_3\}$ be the coordinates of a receiver. Let the vector slip function be $\boldsymbol{d}\, D^{(0)}(\boldsymbol{x},t)$ where $\boldsymbol{d}$ is the constant unit slip vector. Then the far field P-wave displacement along a ray with unit ray vector $\boldsymbol{r}=\boldsymbol{\xi}/R$, where $R = \|\boldsymbol{\xi}\|$, can be written as,

$$u^{(0)}(\xi,t) = A\int_{\Sigma} \dot{D}^{(0)}\left(\boldsymbol{x}, t - \frac{\boldsymbol{x}\cdot\boldsymbol{r} + R}{c}\right) dS \qquad (1)$$

where c is the ray velocity, and the factor A is

$$A = \frac{\mu\Re(\boldsymbol{n},\boldsymbol{d},\boldsymbol{r})}{4\pi\rho c^3 R} = \frac{\mu(n_i d_j + n_j d_i) r_i r_j}{4\pi\rho c^3 R} = \frac{m_{ij} r_i r_j}{4\pi\rho c^3 R}$$

where $\Re$ is the radiation pattern, and m_{ij} is the normalized seismic moment tensor. We band-pass filter both parts of (1) with a filter with central frequency f_0 and cutoff frequencies (f_0-$\Delta f/2$, f_0+$\Delta f/2$), and to identify the filtered versions of (1) we omit the (0) superscript. Therefore the particle velocity at the receiver can be written as:

$$\dot{u}\ (\xi,t) = A\int_{\Sigma} \ddot{D}\left(\boldsymbol{x}, t - \frac{\boldsymbol{x}\cdot\boldsymbol{r} + R}{c} \right) dS \tag{2}$$

Now let us assume that $\dot{u}\ (\ \xi\ ,\ t\ )$ and $\ddot{D}(\boldsymbol{x},t)$ are random functions. This assumption means that we imagine an infinite number of similar faults, or ensemble of faults, all having the same statistical properties of the $\ddot{D}(\boldsymbol{x},t)$ function. (We do not assume here randomness for the direction vectors ***d*** or ***n***.) For our aims it is sufficient that the product $\ddot{D}(\boldsymbol{x},t)\ddot{D}(\boldsymbol{x}+\boldsymbol{y},t+s)$, averaged over an increasingly larger number of sample faults, would converge to some limit $\left\langle \ddot{D}(\boldsymbol{x},t)\ddot{D}(\boldsymbol{x}+\boldsymbol{y},t+s) \right\rangle$, denoted as second moment or covariance. The angular brackets denote "ensemble average", or "mean", that can be visualized as an average over an infinite number of examples/realizations. For the case of zero shift ***y***=0, *s*=0, the covariance is reduced to variance, or mean square $\left\langle \ddot{D}^2(\boldsymbol{x},t) \right\rangle$; for any band-limited function, $\left\langle \ddot{D}(\boldsymbol{x},t) \right\rangle = 0$. We treat the observed records as produced by a particular sample function, or realization, of $\ddot{D}(\boldsymbol{x},t)$, randomly selected from the described ensemble. At sufficiently high f_0 , 5-10 or more times above the corner frequency, this assumption seems to be reasonable for real earthquakes. In this case, a filtered version of an observed record of velocity or acceleration (that corresponds to $\dot{u}(\xi,t)$ or $\ddot{u}(\xi,t)$ in our theory) often looks like a segment of non-stationary random noise.

We believe that it is a reasonable, further assumption that the high-frequency *source* function $\ddot{D}(\boldsymbol{x},t)$ can be treated in the same way. To determine the ensemble mean for the luminosity at the source and for the signal power at the receiver, we consider the product of two equations (2), pertinent to two copies of the finite fault area that are denoted Σ and Σ', computed at the same $\boldsymbol{\xi}$, and we add the $c\rho$ factor to obtain the wave power flux or, briefly speaking, the power $W(\boldsymbol{\xi},t)$, at the receiver

$$W(\xi,t) = c\rho\dot{u}^2(\xi,t) = c\rho A^2 \iint_{\Sigma\Sigma'} \ddot{D}\left((\boldsymbol{x}, t - \frac{\boldsymbol{x}\cdot\boldsymbol{r} + R}{c}) \right) \ddot{D}\left((\boldsymbol{x}', t - \frac{\boldsymbol{x}'\cdot\boldsymbol{r} + R}{c}) \right) dS dS' \tag{3}$$

Now we assume that the concepts of correlation radius, R_c (over the source area), and of correlation time, T_c, can be applied to $\ddot{D}(\boldsymbol{x},t)$. This means, roughly, that within each space-time cell of size $R_c \times R_c \times T_c$, $\ddot{D}(\boldsymbol{x},t)$ is a slowly changing, nearly deterministic, function. In space (along ***x***), it can be assumed to be approximately constant. In time (along *t*), the situation is somewhat more complicated. We assume additionally that the mean source spectrum is slowly changing around f_0, then we can assume that $T_c = 1/\Delta f$. Informally, "slowly changing" means that there are not remarkable spectral features, like spectral spikes or holes, over the pass band, and that the spectral slope in this band is not large; all this does not contradict our knowledge regarding observed spectra (strong-motion or attenuation-corrected teleseismic ones) in the HF range. We can also assume that the correlation time for $\ddot{u}(\xi,t)$ equals T_c as well. We assume Δf of the order of *f*, (like with octave or half-octave filter). Then the autocorrelation of $\ddot{D}(\boldsymbol{x},t)$ along *t* shall represent a small number ($2f_0/\Delta f$) of nearly-sinusoidal swings of frequency about f_0 with the envelope duration about $2T_c$. Correspondingly, with respect to the argument *t*, and over a duration T_c, $\ddot{D}\ (\boldsymbol{x},t)$ can be assumed to be near to a modulated sinusoidal "wavelet" of visual frequency about f_0 with the envelope duration about T_c. For each space-time cell, these wavelets will have particular individual phases and amplitudes. For a random fault model, these phases and amplitudes can be treated as uncorrelated random variates. The introduced space-time cells with a nearly-deterministic behavior of $\ddot{D}(\boldsymbol{x},t)$ within a cell are the main component of our approximate model.

Now let us consider two isochrone surfaces ("sound cones") in 4D (space and time) defined by two close arrival times t-$T_c/2$ and t+ T_c /2; these surfaces enclose between them a definite space-time "layer". If some signal is observed at time *t*, the sound cone must intersect the space-time volume of the earthquake source process. To clarify this situation we give a sketch in Fig 1 that illustrates how the source points contribute to the signal at an arbitrary time *t*. The sketch represents the simplified case of a *linear* (and not planar) earthquake source. The source EE' is located on the X axis in the XY plane; its point H is the hypocenter, where the rupture nucleates. The rupture history is represented by the area S in the *x*-*t* plane. The

receiver, at an arbitrary time, records the sum of all the source effects located on a 3D sound cone CC. The intersection of CC with S gives the line ***ii*** that can be named isochrone. We use this word in a sense that is different from that in Spudich and Frazer (1984), where the isochrone is a line on the fault surface related to the rupture *front*; their isochrone for the case shown in Fig. 1 is the pair of end points of the line ***ii***. For a far-field receiver, the cone CC in the vicinity of the fault degenerates to a plane and ***ii*** becomes a straight line segment.

For a more realistic planar source , sound cones are two 3D objects, and their intersection with the earthquake process volume produces an "isochrone" layer ("thin", with thickness T_c along time axis), with a certain projection onto the spatial fault surface. This projection can be assumed to consist of N_x squares of size $R_c \times R_c$, so that the isochrone volume is approximated as a set of N_x space-time cells. The signals from these cells add up to produce the receiver signal in the interval (t-T_c/2, t+T_c/2). This is how the values of $\dot{u}\ (\xi\ ,\ t\ )$ (as well as $u^{(0)}(\xi, t)$) are formed around the time instant t. Similarly to the case of $\ddot{D}\ (\boldsymbol{x},t)$ over a cell, the values $\dot{u}\ (\xi\ ,\ t\ )$ in time can again be considered as nearly deterministic, over the 1D cell or bin of length T_c around time t, and to represent a short modulated sinusoid. The signal in the mentioned bin will be formed with a certain amplitude and phase, that are the (random) results of summing up signals from every cell of the isochrone layer.

Let us consider the primitive case when summands (contributions from cells) are identical and equal to some D, and the envelope function is a boxcar. Then we have a sum of N_x sinusoids with random phases; and this sum is again a sinusoid whose phase is random and uniform in [0 2π], and whose amplitude is also random with rms value $DN_x^{0.5}$.The randomness of the resulting phase is a very important fact; it implies that the estimation of the observed received power, over small time windows, shall produce highly oscillating results.

A slight improvement can be attained by suppressing the oscillations caused by the "locally sinusoidal" shape of the signal (and preserving the variations of amplitude over time intervals of size T_c and longer). To do this one can use the amplitude of the analytical signal instead of the true receiver signal (that is, to use $\left(\dot{u}\,(\xi\,,t)^2\ +\ \mathrm{H}\left[\dot{u}\,(\xi\,,t)\right]^2\right)^{0.5}$ where H[] is the Hilbert transform over t.) The phase information is lost in this approach, but this loss is absolutely irrelevant in our analysis.

Let us now consider the ensemble means. For the source cell number i, with area $\Delta\Sigma_i$, (equal in our case to R_c^2), we can write its contribution to the mean energy flux at the receiver for and around time t

$$\left\langle \Delta W_i(\boldsymbol{\zeta}, t)\right\rangle \approx\ c\rho A^2\left[\ \int\limits_{\Delta\Sigma_i}\left\langle \ddot{D}^2\left(\ \boldsymbol{x}\ \ ,t-\frac{\boldsymbol{x}\ \cdot\boldsymbol{r}\ +\ R}{c}\right)\right\rangle dS\ \right]\Delta\Sigma_i \tag{4}$$

since we assumed $\ddot{D}\left(\boldsymbol{x}\,,t\right)$ nearly constant over $\boldsymbol{x}$ within $\Delta\Sigma_i$. These contributions are additive at the receiver because we assumed the independence of motion in each of the cells. Now we can introduce the mean P-wave luminosity $\left\langle L\left(\boldsymbol{x}_i\,,t\right)\right\rangle$ through:

$$\left\langle L(\boldsymbol{x},t)\right\rangle\Big|_{\text{on }\Delta\Sigma_i}=\left\langle L_i(\boldsymbol{x}_i,t)\right\rangle=\frac{1}{10\pi\rho c^5}\int\limits_{\Delta\Sigma_i}\left\langle \ddot{D}^2(\boldsymbol{x},t)\right\rangle dS \tag{5}$$

That is, $\left\langle L\left(\boldsymbol{x}_i\,,t\right)\right\rangle$ is a constant over the cell i. In (5), the pre-integral factor is chosen so that its integral over the focal sphere Ω equals unity (we have taken into account that $\int\limits_{\Omega}\Re\,(n_i\,,d_j\,,r_k)\,d\Omega\ =\ {}^2\!/_5$). As a result, both the double integral of $\left\langle L(\boldsymbol{x},t)\right\rangle$ over S and t, and the double integral of the mean energy flux $\left\langle W(\boldsymbol{\xi},t)\right\rangle$, over the surface of the sphere of radius R and t, are equal to the mean seismic energy $\langle E\rangle$ in the frequency band Δf. We note, incidentally, that at a fixed mean square slip acceleration $\left\langle \ddot{D}^2(\boldsymbol{x},t)\right\rangle$, the luminosity (5) is proportional to the area of the cell. This is an important property meaning that the larger is

the correlation radius, the larger, generally, is the radiated HF energy (and also peak acceleration). Expressing $\langle W(\xi,t)\rangle$ through (5) we finally obtain

$$\langle W(\xi,t)\rangle = \frac{5(m_{ij}r_i r_j)^2}{8\pi R^2}\sum_{i=1}^{N_x}\left\langle L_i\left(\boldsymbol{x}_i, t-\frac{\boldsymbol{x}_i\cdot\boldsymbol{r}+R}{c}\right)\right\rangle \Delta\Sigma_i \tag{6}$$

that can be written symbolically as

$$\langle W(\xi,t)\rangle = \frac{5(m_{ij}r_i r_j)^2}{8\pi R^2}\int_{\Sigma}\left\langle L\left(\boldsymbol{x}, t-\frac{\boldsymbol{x}\cdot\boldsymbol{r}+R}{c}\right)\right\rangle dS \tag{7}$$

This is not a true integral, however, because *dS* can never be infinitesimally small. Equation (7) is a generalization of the earlier result of Gusev(1983). Now we can write also the mean cumulative luminosity in P-waves, $\langle L_{cum}\rangle$, for the frequency band Δf:

$$\langle L_{cum}(\boldsymbol{x})\rangle = \int_0^{\infty}\langle L(\boldsymbol{x},t)\rangle dt \tag{8}$$

When considering a particular set of observations (i.e., an individual realization of the random function)we can write similarly:

$$L(\boldsymbol{x},t)\big|_{on\ \Delta\Sigma_i} = L_i(\boldsymbol{x}_i,t) = \frac{1}{10\,\pi\rho\,c^5}\int_{\Delta\Sigma_i}\ddot{D}^2(\boldsymbol{x},t)dS \tag{9}$$

and

$$W(\xi,t) = \frac{5(m_{ij}r_i r_j)^2}{8\pi R^2}\int_{\Sigma} L\left(\boldsymbol{x}, t-\frac{\boldsymbol{x}\cdot\boldsymbol{r}+R}{c}\right)dS \tag{10}$$

The deviations of $L(\boldsymbol{x},t)$ from $\langle L(\boldsymbol{x},t)\rangle$ and of $W(\xi,t)$ from $\langle W(\xi,t)\rangle$ are inevitably large, as already explained. To overcome this difficulty one can smooth the observed $W(\xi,t)$ function within a window of width $T_{sm} > T_c$ and thus reduce the fluctuation noise. The values of the observed $W(\xi,t)$, when sampled with the step T_c, represent independent positive values. One may reduce the fluctuation noise by averaging the observed data over bins of size $T_{sm} > T_c$ (or smoothing them in a similar way). The results will have a smaller coefficient of variation CV than the original values (the estimate for the gain in CV is about $(T_{sm} / T_c)^{0.5}$). However, this approach is of a limited use. The value of T_{sm} must be much smaller than the source process duration *T*, to keep at least a minimal resolution. Unfortunately, with teleseismic observations, the ratio T/T_c is of the order of several tens, and there is no hope to reduce fluctuations significantly. In the following we discuss a workaround that we use to analyze data with large fluctuations.

Luminosity-slip rate correlation and observable time functions

Because of the close analogy between (1) and (10), one can believe that when the named correlation is present, it can be transferred, without any deviation, to a similar correlation between $u^{(0)}(\xi,t)$ and $W(\xi,t)$. Indeed, both (1) and (10) are merely weighted sums of $\dot{D}^{(0)}(\boldsymbol{x},t)$ and of $\ddot{D}^2(\boldsymbol{x},t)$. Let us now assume that the summation of $\dot{D}^{(0)}(\boldsymbol{x},t)$ values is performed on two steps: in the first step, the summation is done within each subarea $\Delta\Sigma_i$, and only afterwards these sums are combined to form the left hand side (LHS) of (1). Let us further assume that the integral of the type (9) for $\ddot{D}^2(\boldsymbol{x},t)$ and an analogous integral for $\dot{D}^{(0)}(\boldsymbol{x},t)$, for a given *i* and a given *t*, can be treated as random variates, and consider their 2×2 covariance

matrix that defines their coefficient of correlation. (Though $\dot{D}^{(0)}(\boldsymbol{x},t)$ is a deterministic object, this is still an acceptable approach because second moments exist for it and its integral). Let us also assume that, apart from a numerical factor, these covariance matrices for different *i* and *t*, are identical. The covariance matrix of a sum is a sum of covariance matrices of summands. For this reason, after summation over *i* and averaging over *t*, the result (a sample value of smoothed $W(\xi,t)$ and a similarly smoothed value of $u^{(0)}(\xi,t)$) will have the covariance matrix that is similar to such matrix of any summand, and thus the same coefficient of correlation. We can conclude that the correlation coefficient between wave displacement and mean wave power flux truly represents the similar coefficient between slip rate and mean luminosity.

However this result holds for the ideal case only. With observed data, we shall estimate the correlation coefficient from a fluctuating signal. In this case, the result will inevitably be biased. We reiterate that these fluctuations are caused by the inevitable oscillations of amplitude of a band-limited signal, that take place even when the mean signal power is strictly constant. The fluctuations will result in errors in the estimates of the variance-covariance. These errors will have positive or negative sign, and, generally, might compensate each other, for example in multiple-recorder averaging. Nevertheless their effect on the observed correlation coefficient will be asymmetric: the high values of the correlation coefficient will in most cases be reduced. This is evident for a model case of two copies/realizations of a segment of slightly non-stationary random signal (with constant mean power). In this case, the "ideal"coefficient of correlation between squared *mean* amplitudes is automatically equal to unity; whereas for any actual pair of *realizations*, this coefficient will be less than unity.

Let us now consider in more detail the already mentioned correlation coefficients: the "ideal" (ensemble mean) correlation coefficient ρ_{id}; the observed coefficient ρ_{ob}; and the maximum potential observable coefficient ρ_{obmax}, corresponding to the unity value for the case of the ensemble mean. Our final aim is to determine ρ_{id} knowing ρ_{ob}, and, for this purpose, to know the value of ρ_{obmax} can be useful. To determine ρ_{obmax}, we take the long-period signal $u^{(0)}(t)$ and use it as the envelope function for a hypothetic power signal *W(t)*. Using this prescribed envelope, we simulate a number of realizations (say, 25) of band-passed nonstationary noise (each of them appears like $\dot{u}(t)$). From these 25 artificial data we determine the average correlation between the squared result and the initial $u^{(0)}(t)$ function, and consider it as an estimate for ρ_{obmax}.

With ρ_{ob} and ρ_{obmax} values at hand, we could estimate ρ_{id}, provided we can establish a theoretical relationship among ρ_{ob}, ρ_{obmax} and ρ_{id}. In order to find such a relationship we shall construct a simple model of fluctuating signal. Let us consider a random vector $\boldsymbol{a}=\{a_i\}$ whose components describe the sequences of (positive) amplitudes of $u^{(0)}(t)$; the components a_i have the same distribution and they can be mutually correlated in some irrelevant way. To represent the different degrees of correlation between $u^{(0)}(t)$ and $\dot{u}^2(t)$ we introduce another vector $\boldsymbol{b}$, with the same dimension as $\boldsymbol{a}$ but statistically independent from $\boldsymbol{a}$, and form the vector $\boldsymbol{d}_0$, defined as a weighted sum of $\boldsymbol{a}$ and $\boldsymbol{b}$:

$$\boldsymbol{d}_0=c\boldsymbol{a}+(1-c)\boldsymbol{b}=c\boldsymbol{a}+p\boldsymbol{b}$$

where *c* defines the degree of correlation ($0<c<1$)and $p=1-c$.

The pair of vectors $(\boldsymbol{a},\boldsymbol{d}_0)$ represents "ideal" observations for the case of limited correlation. It is easy to see that the correlation coefficient between $\boldsymbol{a}$ and $\boldsymbol{d}_0$ is

$$\mathrm{Corr}(a,d_0)=\frac{\mathrm{Cov}(a,d_0)}{(\mathrm{Var}(a)\,\mathrm{Var}(d_0))^{0.5}}=\frac{c}{(c^2+p^2)^{0.5}} \tag{11}$$

It varies between unity when $c=1$ and zero when $c=0$, as could be expected. To imitate the formation of random fluctuations of a certain size, we multiply $\boldsymbol{d}_0$ by a random factor obtaining:

$$\boldsymbol{d}=\boldsymbol{d}_0(1+k\boldsymbol{s}) \tag{12}$$

where $\boldsymbol{s}$ is a random vector of the same size as $\boldsymbol{a}$, with zero mean, and *k* is a "spoiling" coefficient that defines the relative level of the fluctuations. With $k=0$, we return to the "ideal" case. In the non-ideal case, one can show that

$$\mathrm{Corr}(\ a, d\ ) = \frac{c}{\left\{(c^2 + p^2) + k^2\ \mathrm{Var}(\ s)[\,c^2 + p^2 + \langle a \rangle^2 / \mathrm{Var}(\ a)]\right\}^{0.5}} \qquad (13)$$

We further assume that ***a*** and ***b*** are distributed exponentially; this is accurate for the amplitude of the analytical signal formed from Gaussian noise, and such a representation is adequate for our aims. This gives

$$\mathrm{Corr}(a,d) = \frac{c}{\left[c^2 + p^2 + z(c^2 + p^2 + 1)\right]^{0.5}} \qquad (14)$$

where we denoted z the unknown combination $k^2/\mathrm{var}(\boldsymbol{s})$ .We shall use formula (14) in two ways. First, we can deduce the value of z from ρ_{obmax} setting c=1; and, second, with the z value at hand, we can deduce the unknown c value (and thus ρ_{id} value) from ρ_{ob}.

Compensating for scattering of HF waves

One additional complication in our data analysis is caused by the distortion of the signal along the path to the station. Whereas the displacement P-wave waveform can be treated relatively safely as if it was radiated in a homogeneous medium, high-frequency signal is significantly distorted by scattering and multipathing, as always seen in the formation of P-wave coda. Since the incoherent energy is additive, this process is linear *for power*, and can be described by the convolution of power time histories (strictly, for ensemble averages):

$$W_s(\cdot) = W_o(\cdot) * W_h(\cdot) \qquad (15)$$

where $W_s(t)$, $W_o(t)$ and $W_h(t)$ are the power (squared high-frequency amplitude) time histories for, respectively: signal at a station; signal at the source for the particular ray directed to the station, and for the "power Green's function of the medium" for the same particular ray. All these correspond to a particular moment tensor orientation of the source, to a particular component at the station and to a particular frequency band. To recover $W_o(t)$ from the observations, Gusev and Pavlov (1991) proposed to consider the convolution with W_h (t) as a filter, to construct the corresponding inverse filter $W_h^{-1}(\cdot)$ from a record of an aftershock with similar moment tensor orientation and to apply this inverse filter to $W_s(\cdot)$. This procedure has been successfully applied to recover first and second time moments of records of two large earthquakes, and further to determine the centroid and the size of the HF earthquake sources. However this procedure is less reliable when applied to reconstruct details of $W_o(t)$, because the result of the inversion depends, to some degree, on the choice of the stabilizing constraints used in the inversion. Thus, when using such waveforms for the study of the correlation one has difficulties in producing really convincing result.

In the present study, because of its specific purpose, we use another approach. To obtain comparable low- and high-frequency signals, we artificially distort low-frequency signal by convolution with an operator that imitates $W_h(t)$. Then we can determine the correlation between comparable objects: artificially distorted low-frequency signal and naturally distorted raw high-frequency signal. At first, we made attempts to determine an usable approximation to $W_h(t)$ by averaging high-frequency squared records of smaller, short-duration, intermediate-depth earthquakes (M=5.0-5.6), but found out that these records contain too much noise to perform reliable averaging. We then took another approach and selected a number of records of earthquakes with M=5.8-6.2, with relatively short durations of 2-3 s. Using the formula (15) and approximating $W_o(t)$ with the displacement pulse, we select, by trial and error, a credible analytical representation of $W_h(t)$, common to all stations and earthquakes. This artificial signal is then applied to modify each low-frequency record.

DATA SET AND ITS PROCESSING

To compare observed far field displacement and power time functions, we need clear isolated body wave signals with sufficiently high signal to noise(S/N) ratio over a sufficiently wide frequency band. From each "raw" GDSN BB record we reconstruct the time histories for displacement and for squared, high-frequency

band-filtered, velocity, or "power". These time histories, after smoothing and decimation, can be used to analyze the slip rate-luminosity relationship at the source.

An important practical step is the selection of signals with clear, one-sided (positive or negative) displacement time history. This type of signal is theoretically predicted for a planar shear source (double-couple source). Intermediate-depth earthquake sources mostly follow this model. Despite a considerable number of deviations, we have been able to select a considerable number of events whose mechanism is sufficiently near to plane shear. To collect data we initially selected all earthquakes in the IRIS DMS database since 1990 with $M_w \geq 6.8$ and focal depth H=90-200 km. P-wave groups on broad-band vertical (BHZ) channels (sampling interval Δt_0=0.05 s) of GDSN stations at epicentral distances from 25° to 100° have been retrieved through the IRIS DMS center. At first, for each of the 31 events we have initially selected, 5-10 P-wave records, with acceptable S/N ratio, have been analyzed. For intermediate-depth events, typically no overlapping of P-wave and pP-wave groups can be expected, but the actual situation depends on the particular combination of source depth and source duration. The events for which the *P* and *pP* groups are not suffuciently separated have been discarded. In the case of a simple double-couple source, P-wave displacement should appear as unipolar (one-sided) pulse. However, for a considerable fraction of events there is a large proportion of records (non-nodal) that are not one-sided, manifesting complex ruptures. These cases have also been omitted from our data. The remaining 23 events have been kept for further study (Table 1). For these events, additional records have been retrieved. We selected a common upper cutoff frequency for analyzing all events and records, on the basis of the actual signal to noise S/N ratios. We found out that despite a number of favorable cases (stations in central parts of continents), the highest usable frequency is typically 2.5-3 Hz. Thus we selected 2.5 Hz as the common upper cutoff. When forming a set of records for a particular event, we applied the following rules:

1. the *S/N* ratio is no less than 2-3 at 2.5 Hz ;
2. for each group of near stations, that have recorded similar waveforms, only one is selected;
3. near-nodal records are rejected.

As a result, we keep from 5 to 18 records per station. These records are taken from the BHZ channel, deconvolved for the channel transfer function and for the attenuation operator, with t^*=0.5 (with phase correction). The result represents an initial velocity record. To form a well-defined displacement signal, the initial record is low-pass filtered with a zero-phase filter with 0.7 Hz upper cutoff, and then integrated, to produce an empirical estimate of $u^{(0)}(t)$, that we further denote with $m(t)$. To form the receiver "power" signal, the initial record is filtered with a zero-phase band-pass filter with cutoffs at 0.5 and 2.5 Hz, and the squared analytical signal is formed, giving an empirical estimate of $\dot{u}^2(t)$, that we denote as $p(t)$. Then we perform smoothing of $m(t)$ and $p(t)$, using the time window of boxcar shape, with the width Δt that has been selected on a case by case basis, but typically about 0.8s; Δt is always a multiple of the initial time step 0.05 s. The results were decimated with the time step Δt, producing two sequences of statistically independent consecutive average amplitude values denoted with m_i, and p_i.

To select the $W_h(t)$ function, several earthquakes with M_w=5.8-6.2 are analyzed. Fig 2 shows four examples. One can see the "power" signal p_i, the displacement signal m_i, and the modified displacement signal that will be denoted by q_i, obtained by convolution with the following representative or typical shape function (arbitrary scale):

$$W(t) = 1000t\exp(-t/0.1) + [1.0t\exp(-t/1.5)]^{0.3} \tag{16}$$

The shape (16) has been determined by trial and error on the basis of the qualitative analysis of about 50 records, at different stations, of eight earthquakes. One could expect that for intermediate-depth sources, the scattering effect is mostly related to the vicinity of the receiver and thus will be specific for a station. Such a behavior, if it exists, must be rather moderate: the variations of P-wave coda amplitude between individual records at the same station, seem to be of the same order as between two stations. One can see in Fig. 2 that sometimes the assumed "average" $W_h(t)$ shape produces a quite nice fit to the data; in other cases it may somewhat underestimate or overestimate the scattering-related bias.

During the main stage of the data processing, for each analyzed record, the following procedure has been followed:

(1) application of the instrument and attenuation correction, filtering, and calculation of the power (as explained above) to produce the two traces $m(t)$ and $p(t)$;

(2) selection of the onset time, common to $m(t)$ and $p(t)$, by visual inspection of both traces;
(3) definition of the end time for $m(t)$, by visual inspection, using as criterion the return of the trace to the zero line (the individual values of duration d_m obtained in this way vary between 6 and 20 s);
(4) selection of the end time for $p(t)$, by visual inspection, either when the P-coda level becomes small or, more often, just before pP onset;
(5) convolution of $m(t)$ with the assumed $W_h(t)$to obtain the modified displacement $q(t)$; selection of the end time of $q(t)$ identical to that of $p(t)$, and determination of the duration parameter d_p;
(6) using the preset common integer parameter k_0=16, determination of the time unit $\Delta t=\Delta t_0$(Integer (d_m/k_0)+1), and the final number of time bins k_1=Integer (d_p /Δt) slicing the already isolated $m(t)$, $q(t)$ and $p(t)$ pulses in k, k_1 and k_1 identical time bins of duration Δt, and averaging each function over each bin; the resulting time sequences are denoted m_i, q_i and p_i;
(7) calculation of the coefficients of correlation ρ_{ob} between q_i and p_i, (and also ρ_{ob0} between m_i and p_i over only k segments, for comparison);
(8) generation of N_{sim}=25 realizations of 0.5-2.5 Hz band-limited noise, and construction of simulated HF signals, using $q(t)$ as an envelope function; step 6 is then applied to produce simulated "power" traces $p_{sim}(t)$, and simulated sequences $p_{sim,i}$; step 7 is applied to calculate N_{sim} variants of the correlation coefficient ρ_{sim} between q_i and $p_{sim,i}$; from N_{sim} values of ρ_{sim}, determination of the average ρ_{simav} and of its standard deviation s_{sim} (we believe that ρ_{simav} is a good estimate for ρ_{id} that gives an upper limit for ρ_{ob});
(9) calculation of the Student's t-value $(\rho_{simav} - \rho_{ob})/s_{sim}$ to judge the significance of the difference between ρ_{ob} and ρ_{simav}.

In Fig 3 we show a number of random realizations of the noise-like signal generated from the same $q(t)$ function, and the actual $p(t)$ function. The variability of noise realizations is significant but still limited, and the actual observed $p(t)$ looks different from any of the noise realizations. The entire processing sequence is illustrated in Fig 4.

RESULTS AND THEIR ANALYSIS

In Table 1, the list of the analyzed earthquakes is given. In Table 2 we give an example of the results for several records of the same event (No.20 in Table 1). In Table 3 we give the average results for all studied earthquakes. The main results can be summarized as follows.

1. Source durations typically vary from 12 to 25 s, resulting in Δt values of 0.7-1.5 s. To unravel the presence of possible noise in the values of p_i after smoothing over the window of such a duration, it is appropriate to observe that the correlation time for our HF data is near to the inverse of the frequency bandwidth, or about 0.5 s, so that the number of degrees of freedom per single p_i value is very low (1.5-3). This means that p_i values must have a significant scatter, and just this is seen on the simulations of Fig 3. For this reason, it is indeed critical to apply formal statistical analysis in order to determine whether the correlation between q_i and p_i is comparable or significantly lower than the similar correlation between q_{simi} and q_i.
2. The values of ρ_{ob} for individual records of a single earthquake vary significantly, but are systematically lower than ρ_{sim}. The standardized difference t (Student's value) varies significantly, and typically is around 2.3, giving significance levels between 20% (or more) and 0.1%, and typically about 5%. Since each record gives an independent observation, these probabilities from individual records of the same event must be multiplied to give the joint significance level. It is evidently very low, so that the statement "ρ_{ob} is below ρ_{sim}" can be considered true even for the data of a single earthquake. The data of the whole set of earthquakes makes this conclusion proven.
3. The values of ρ_{sim} are rather stable, of the order of 0.7, and they indicate that the lack of close visual or formal correlation between q_i and p_i or between $q(t)$ and $p(t)$ is the result of the properties of the data, and must be a general rule for our combination of bandwidth and duration, irrespectively of the degree of correlation between q_i and the unobservable mean p_i. Only the *degree* of correlation (or, maybe better to say, decorrelation) has a physical meaning.
4. Average ρ_{ob} values of individual earthquakes fall in a relatively narrow range 0.35-0.65. The average over all earthquakes is 0.52, and it can be taken as the lower limit for the "ideal" correlation coefficient, ρ_{id}, for any earthquake.

In Fig 5 we give examples of m_i , q_i , and p_i sequences for four records of different earthquakes, with high and low levels of correlation. Case (b) is anomalous; it not only has the lowermost ρ_{ob} value, but its

record look merely paradoxical because one or more bursts of HF energy occurs during the time interval of near-zero slip rate. Our preliminary explanation is that this earthquake caused a short series of low moment, very high-stress-drop aftershocks with a very small delay with respect to the main shock. The tendency of HF energy bursts to appear just near the end or even slightly later than the visual end of a displacement pulse was seen also in other cases, though not so prominently.

To roughly estimate the "true" coefficient of correlation between mean power and displacement (assumedly equal to the "true" coefficient of correlation between slip rate and luminosity at the source), we first use Eq. 14 with c=1 for the case of simulated data, and assume there $Corr(a,d)$ to be equal to the average ρ_{obmax}=0.72. Solving with respect to z we obtain the estimate z = 0.46. We can now set it in (14), and assuming in the right-hand side of (14) $Corr(a,d)= \rho_{ob}$ = 0.52 (average value), we can resolve (14), with respect to c, and obtain c=0.57. From (11) we now determine average estimate $Corr(a,d_0)= \rho_{id}$ =0.80. By means of the same procedure, starting from the interval of station averages for individual events ρ_{ob}=[0.35-0.65], we obtain the estimate of range for ρ_{id} values of individual events as [0.54-0.96]. These values represent our final results regarding true (ensemble-mean) values of the correlation coefficient both for the record and for the source.

DISCUSSION

The average value of the correlation coefficient ρ_{ob} =0.52 is the observed average value for a particular combination of source duration range and frequency band. Variations of ρ_{ob} between individual earthquakes, from 0.35 to 0.65, indicate genuine differences between earthquakes. These figures agree with the intuitive understanding that can be acquired from visual inspection of seismograms obtained by several simultaneously working channels with different passband. The deviation of these values from unity has two components: genuine difference between slip rate and mean luminosity, and random fluctuations. As the effect of these fluctuations is excluded from the "ideal" correlation values ρ_{id}, the "ideal" average value ρ_{id}=0.80 and the range 0.54-0.96 reflect intrinsic properties of the radiating faults. These values mean that although the decorrelation between the slip rate and mean luminosity is typically present, the degree of this decorrelation is moderate.

An important question is whether our results obtained for intermediate earthquakes can be extrapolated to shallow earthquakes whose properties may be of much broader geophysical and practical importance. We are unaware of any evidence that the physical mechanisms of shallow and intermediate earthquakes are different: both populations are shear dislocations with, generally similar source spectra, and the typically noted difference of average stress drop value is quantitative, not qualitative. This makes it reasonable the idea that the general conclusion of this paper – that low-frequency low-wavenumber motion and high-frequency high-wavenumber motion at the source are correlated only up a limited degree – can be transferred to the case of shallow earthquakes. We believe that even our numerical estimate ρ_{id}=0.80 can be taken as a starting approximation for shallow earthquakes. This value can be treated as a constraint that should be imposed on the simulated local source slip rate and simulated local *mean* luminosity, in order to represent realistically the wide-band source radiation. Simulated mean luminosity is of course the average over the realizations obtained in a series of simulations. For a single realization of luminosity, the expected correlation is much lower, like 0.52 in our case.

CONCLUSIONS

1. A data processing procedure is developed that is suitable for the study of the correlation between displacement and high-frequency (HF) power in the teleseismic P-wave signal. In this procedure we considerably suppress the bias related to the formation of HF P coda through scattering.
2. Having analyzed 344 teleseismic records of 23 intermediate-depth earthquakes, we found that the correlation between time histories of displacement and HF (0.5-2.5Hz) power is limited, with the average coefficient of correlation equal to 0.52; the range of averages over the records of individual earthquakes varies from 0.35 to 0.65.
3. Although the decreased correlation property is partly an evident effect of the random, stochastic nature of HF waves, this explanation is incomplete. We show statistically that there is also a highly significant contribution of "true" decorrelation between displacement and mean (ensemble-average) HF energy.

Estimated values for the mean coefficient of correlation are: the average over events: 0.80, the range for individual earthquakes: from 0.54 to 0.96

4. Our estimates of the coefficient of correlation between displacement and high-frequency (HF) power in P-wave signal can be transferred without change to the correlation between local source slip rate and local P-wave luminosity (or radiated power flux) for the same spot of the fault.

5. The results suggest a limited correlation between slip rate and HF power also for shallow earthquakes.

ACKNOWLEGEMENTS

Fruitful discussions with Fabio Romanelli are here acknowledged. This work is a contribution to the Italian MIUR-COFINANZIAMENTO projects 2001045878_007 and 2002047575_002.

REFERENCES

Blandford, R. R. 1975. A source theory for complex earthquakes Bull. Seismol. Soc. Amer., 65, 1385 – 1405.

Boatwright, J., 1982. A dynamic model for far-field acceleration, Bull. Seismol. Soc. Amer., 72, 1049-1068.

Boatwright, J., 1988.The seismic radiation from composite models of faulting, Bull. Seismol. Soc. Amer., 78, 489 - 508

Papageorgiou, A.S. and K. Aki.1983. A specific barrier model for the quantitative description of inhomogeneous faulting and the prediction of strong ground motion. Part I: Description of the model, Bull. Seismol. Soc. Amer., 73, 693-722.

Gusev, A. A. 1983. Descriptive statistical model of earthquake source radiation and its applicability to an estimation of short-period strong ground motion, Geophys. J. R. Astron. Soc. 74, 787-800.

Gusev A.A. 1989. Multiasperity fault model and the nature of short-period subsources. Pure Appl. Geophys, 130, 635-660.

Gusev, A. A. and V. M. Pavlov, Deconvolution of squared velocity waveform as applied to study of non-coherent short-period radiator in earthquake source, Pure Appl. Geophys. 136, 236-244, 1991.

Gusev, A. A. and V. M. Pavlov. 1998. Preliminary determination of parameters of the high-frequency source for the Dec 05, 1997 Mw=7.9 Kronotsky earthquake. In: XXVI Gen. Assembly, Eur. Seismol. Comission, Papers, Tel-Aviv, Israel, pp 73-77

Iida M. and M. Hakuno 1984 The difference in the complexities between the 1978 Miyagiken-oki earthquake and the 1968 Tokachi-oki earthquake from a viewpoint of the short-period range. J. Natur. Disaster Sci., 6, 1-26

Hanks, T.C. 1979. b values and $\omega^{-\gamma}$ seismic source models: Implication for tectonic stress variations along active crustal fault zones and the estimation of high-frequency strong ground motion. J. Geophys. Res., 84, 2235–2242.

Heaton, T. H., 1990. Evidence for and implications of self-healing pulses of slip in earthquake rupture, Phys. Earth Planet Int., 64, 1-20,.

Kakehi, Y., and K. Irikura, 1996. Estimation of high frequency wave radiation areas on the fault plane by the envelope inversion of acceleration seismograms, Geophys. J. Int., 125, 892--900,.

Nishimura, T., H. Nakahara, H. Sato, and M. Ohtake, Source process of the 1994 far east off Sanriku earthquake, Japan, as inferred from a broad-band seismogram, Sci. Rep. Tohoku Univ. 34, 121-134, 1996.

Spudich, P., and L.N. Frazer, 1984. Use of ray theory to calculate high-frequency radiation from

earthquake sources having spatially variable rupture velocity and stress drop, Bull. Seismol. Soc. Amer., 74, 2061-2082,.

Zeng, Y., K. Aki and T.-L. Teng 1993. Mapping of the high frequency source radiation for the 1989 Loma Prieta Earthquake, California, J. Geophys Res. 98, 11981-11993.

Table 1. Parameters of the earthquakes used for the study.

No	Date	Time	Lat. °	Long.°	Depth, km	M_w	N_{sta}
1	1990/07/27	12:37:59.5	-15.35	167.46	125	7.2HRV	4
2	1993/01/15	11:06:05.9	43.30	143.69	102	7.6HRV	7
3	1993/05/24	23:51:28.2	23.23	-66.63	221	7.0NEIC	9
4	1993/08/09	12:42:48.1	36.37	70.86	214	7.0HRV	9
5	1994/02/11	21:17:31.1	-18.77	169.16	205	6.8HRV	10
6	1995/06/29	12:24:03.2	-19.54	169.28	139	6.6HRV	7
7	1995/10/21	02:38:57.1	16.84	-93.46	159	7.2HRV	10
8	1995/12/25	04:43:24.4	-6.90	129.15	141	7.1HRV	11
9	1996/04/16	00:30:54.6	-24.06	-177.03	110	7.2HRV	8
10	1997/05/03	16:46:02.0	-31.79	-179.38	108	6.9HRV	15
11	1997/09/02	12:13:22.9	3.85	-75.75	198	6.8HRV	9
12	1997/10/14	09:53:18.1	-22.10	-176.77	167	7.7HRV	9
13	1997/10/28	06:15:17.3	-4.36	-76.68	112	7.2HRV	8
14	1997/11/15	18:59:24.3	-15.14	167.37	123	7.0HRV	14
15	1998/01/04	06:11:58.9	-22.30	170.91	100	7.5HRV	6
16	1998/07/09	14:45:39.9	-30.48	-178.99	129	6.9HRV	12
17	1998/07/16	11:56:36.4	-11.04	166.16	110	7.0HRV	11
18	1998/12/27	00:38:26.7	-21.63	-176.37	144	6.8HRV	17
19	1999/02/06	21:47:59.4	-12.85	166.69	129	7.3HRV	10
20	1999/04/05	11:08:04.0	-5.59	149.57	150	7.4HRV	18
21	1999/05/10	20:33:02.0	-5.15	150.88	134	7.1HRV	19
22	2000/03/28	11:00:22.5	22.33	143.73	163	7.6HRV	18
23	2000/05/12	18:43:18.1	-23.54	-66.45	225	7.2HRV	10

N_{sta} - number of records processed for each event

Table 2. Results of the processing for the event 990206 (No.19) for all 10 stations; the broadband vertical (BHZ) channel.

sta.	d_m ,s	d_p , s	k_1	Δt, s	ρ_{ob0}	ρ_{ob}	ρ_{simav}	σ_{sim}	t_{St}
anmo	14.6	17.3	18	0.95	0.14	0.32	0.74	0.092	-4.54
bjt	6.0	12.7	33	0.35	0.36	0.25	0.72	0.121	-3.82
brvk	15.3	15.6	16	0.95	0.02	0.24	0.64	0.156	-2.57
cola	10.5	15.7	23	0.65	-0.17	0.00	0.68	0.133	-5.12
ctao	10.4	13.0	19	0.65	0.07	0.35	0.64	0.090	-3.29
kurk	11.7	14.2	19	0.75	0.84	0.86	0.75	0.105	1.05
pfo	13.7	15.6	18	0.85	0.46	0.55	0.70	0.100	-1.51
tly	8.7	11.6	21	0.55	0.20	0.35	0.67	0.109	-2.96
uln	7.4	11.8	25	0.45	0.50	0.46	0.69	0.134	-1.69
yak	8.0	11.9	23	0.50	0.28	0.31	0.67	0.123	-2.92
average	10.6	13.9	22	0.66	0.27	0.37	0.69	0.116	-2.73
st.dev.	3.1	2.0	5	0.21	0.29	0.23	0.04	0.021	1.74

d_m and d_p : visually selected durations for the displacement pulse and the 0.5-2.5 Hz power pulse; k_1: number of time bins within the duration of T_p; Δt: size of a time bin; ρ_{ob0} - correlation coefficient determined from m_i and p_i over k_0=16 bins (for reference only, further not used), ρ_{ob}: same, determined from q_i, and p_i over k_1 bins; ρ_{simav} and σ_{sim}: average coefficient of correlation over 25 simulated p_{simi} sequences, and empirical standard deviation over each group of 25 values, t_{St} – Student's *t*-statistic for testing the hypothesis $\rho_{ob} < \rho_{simav}$ ($t_{St} = (\rho_{simav} - \rho_{ob})/\sigma_{sim}$)

Table 3. Results of the calculation for each of the 23 earthquakes.

No.	Event	ρ_{ob} $\sigma\rho_{ob}$	ρ_{ob} $\sigma\rho_{ob}$	ρ_{simav} $\sigma\rho_{simav}$	t_{St} σt_{St}
1	900727	0.31	0.48	0.728	-2.94
		0.23	*0.081*	*0.033*	*1.514*
2	930115	0.37	0.51	0.749	-3.058
		0.31	*0.205*	*0.058*	*2.814*
3	930524	0.37	0.508	0.66	-1.541
		0.19	*0.129*	*0.063*	*1.121*
4	930809	0.28	0.418	0.743	-3.585
		0.20	*0.232*	*0.048*	*2.718*
5	940211	0.48	0.604	0.73	-1.4
		0.31	*0.208*	*0.057*	*2.014*
6	950629	0.35	0.411	0.721	-2.997
		0.22	*0.242*	*0.062*	*2.946*
7	951021	0.46	0.543	0.788	-3.32
		0.20	*0.188*	*0.049*	*3.332*
8	951225	0.52	0.622	0.748	-1.261
		0.22	*0.175*	*0.066*	*1.908*
9	960416	0.47	0.514	0.72	-1.762
		0.40	*0.355*	*0.04*	*2.831*
10	970503	0.47	0.351	0.697	-3.226
		0.34	*0.292*	*0.069*	*2.666*
11	970902	0.47	0.629	0.731	-1.07
		0.25	*0.129*	*0.052*	*1.371*
12	971014	0.49	0.558	0.773	-2.763
		0.22	*0.275*	*0.079*	*2.7*
13	971028	0.58	0.629	0.739	-0.976
		0.15	*0.128*	*0.044*	*0.903*
14	971115	0.44	0.541	0.735	-1.936
		0.28	*0.218*	*0.032*	*2.259*
15	980104	0.64	0.615	0.77	-1.49
		0.19	*0.206*	*0.083*	*1.68*
16	980709	0.39	0.477	0.708	-2.208
		0.26	*0.274*	*0.055*	*2.153*
17	980716	0.36	0.522	0.66	-1.112
		0.35	*0.209*	*0.032*	*1.759*
18	981227	0.38	0.464	0.666	-1.853
		0.35	*0.244*	*0.068*	*2.474*
19	990206	0.27	0.369	0.691	-2.739
		0.29	*0.225*	*0.038*	*1.748*
20	990405	0.39	0.456	0.753	-3.693
		0.20	*0.145*	*0.050*	*2.571*
21	990510	0.566	0.561	0.700	-1.281
		0.24	*0.272*	*0.038*	*2.466*
22	000328	0.31	0.502	0.679	-1.838
		0.36	*0.302*	*0.053*	*3.20*
23	000512	0.48	0.548	0.718	-1.554
		0.27	*0.245*	*0.025*	*2.125*
	average	0.427	0.514	0.7220	-2.1567
	st.dev.1	0.096	0.079	0.0355	0.8824
	st.dev.2	*0.261*	*0.216*	*0.0519*	*2.2293*

The values ρ_{ob0}, ρ_{ob}, ρ_{simav}, and t_{St} are averages over stations processed for each earthquake, and correspond to the lowest but one line of Table 2. In the main part of the table, two lines are given for each earthquake, the upper one contains mean values over N_{sta} records, and the lower one, italicized, contains standard deviations obtained in averaging over several records of the same earthquake. The three lowermost lines contain: *average* over events (i.e. over station averages), standard deviation *st.dev.*1 among events, and *st.dev.*2 - average over "within-event" standard deviations (italicized), respectively.

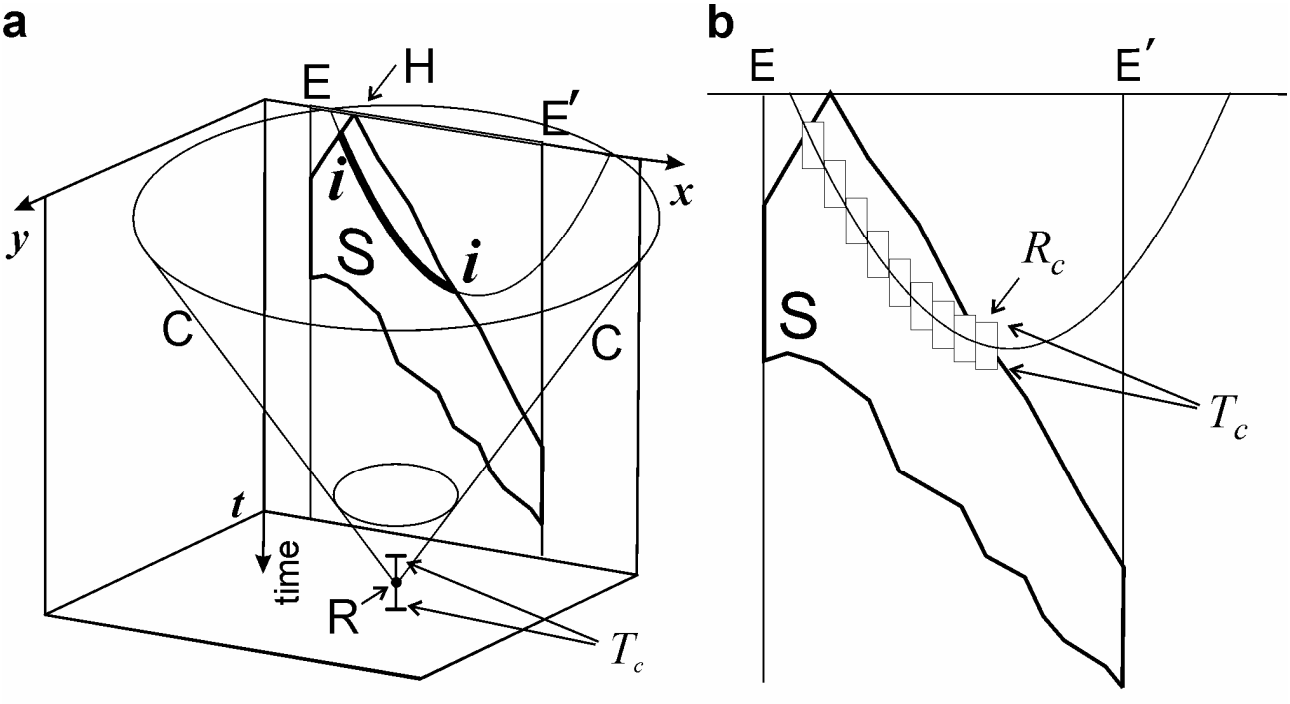

Figure 1. Formation of the body wave high-frequency power flux signal for the case of a linear earthquake source: a – in the 3D space (x,y,t), b – the detail of a in the (x,t) plane . The source occupies the segment EE' of the x axis, and the time axis increases downward. In a, the observation space-time point is R, and it corresponds to a particular time t. CC is a "sound cone", i.e. the surface over which the signal received at R can be generated. The hypocenter or nucleation point is denoted by H, and the area S is the space-time area of the earthquake source process. CC and S intersect along the isochrone ii, where the signal received at R is generated. The vertical segment at R depicts the finite time window over which an individual meaningful estimate of the received power can be made; its length is equal to the signal correlation time T_c. In b we illustrate that the mentioned estimate can seen as formed by independent contributions from the space-time cells, with cell dimensions T_c along time, and R_c along x, situated along the isochrone.

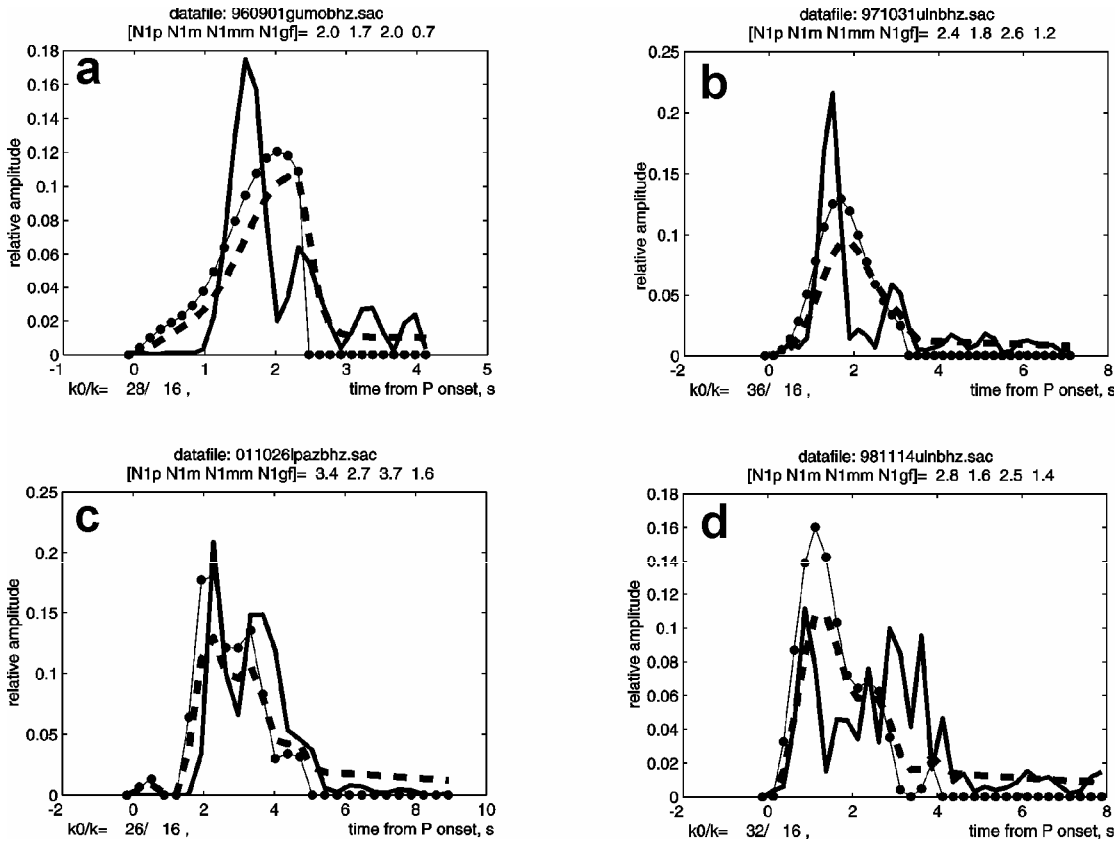

Figure 2. Illustration to the performance of the selected typical medium power response shape function (16). The convolution procedure is applied to P-wave records of M=6 earthquakes. Solid line: power in the 0.5-2.5 Hz band; dots: displacement; dashes: predicted power signal, constructed through the convolution of the displacement signal with the pulse of the selected shape (16) that assumedly emulates the response of the medium. Real HF pulses including codas are generally comparable with the predicted ones, but with large deviations.

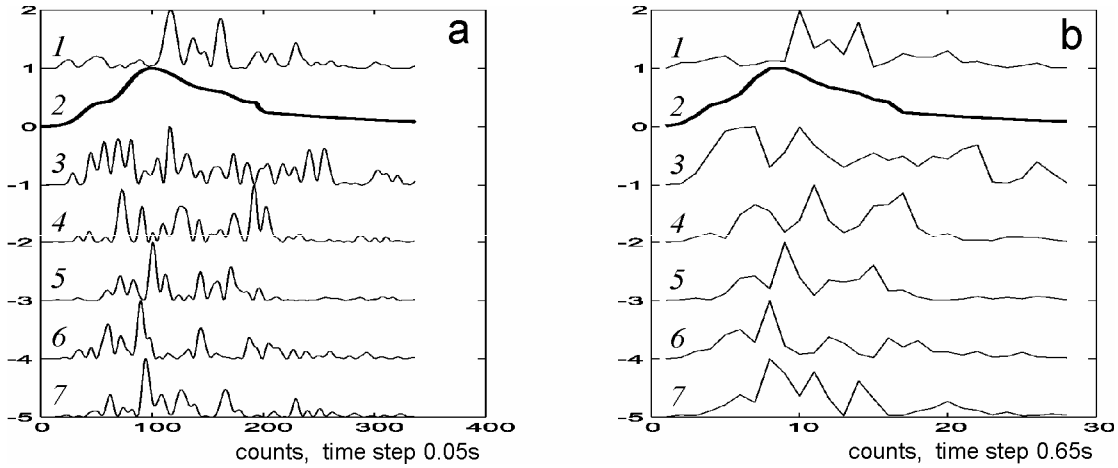

Figure 3. Illustration of the procedure used to estimate the significance of the displacement-power correlation. a: signals with original time step 0.05 s: "raw" HF power $p(t)$ signal (1), modified displacement $q(t)$ (2), and simulated HF power $p_{sim}(t)$ (five realizations 3-7), for the event 000328 recorded at the station PFO. b: smoothed and decimated variant of the same functions (denoted p_i; q_i; $p_{sim,i}$.) with the time step Δt=0.65 s (averaging by 13 points). Averaging in this way gives about 1.5 degrees of freedom for each data point in b, because $T_c \approx \Delta f^{-1}=(2.5\text{-}0.5)^{-1}=0.5$ s. All intuitively significant variations of the data shown in a are preserved in b. The variability among the random realizations (3-7) is well-expressed, yet the actual observed signal (1) looks different from any of them, illustrating that the lack of correlation between (1) and (2) cannot be ascribed solely to the random fluctuations.

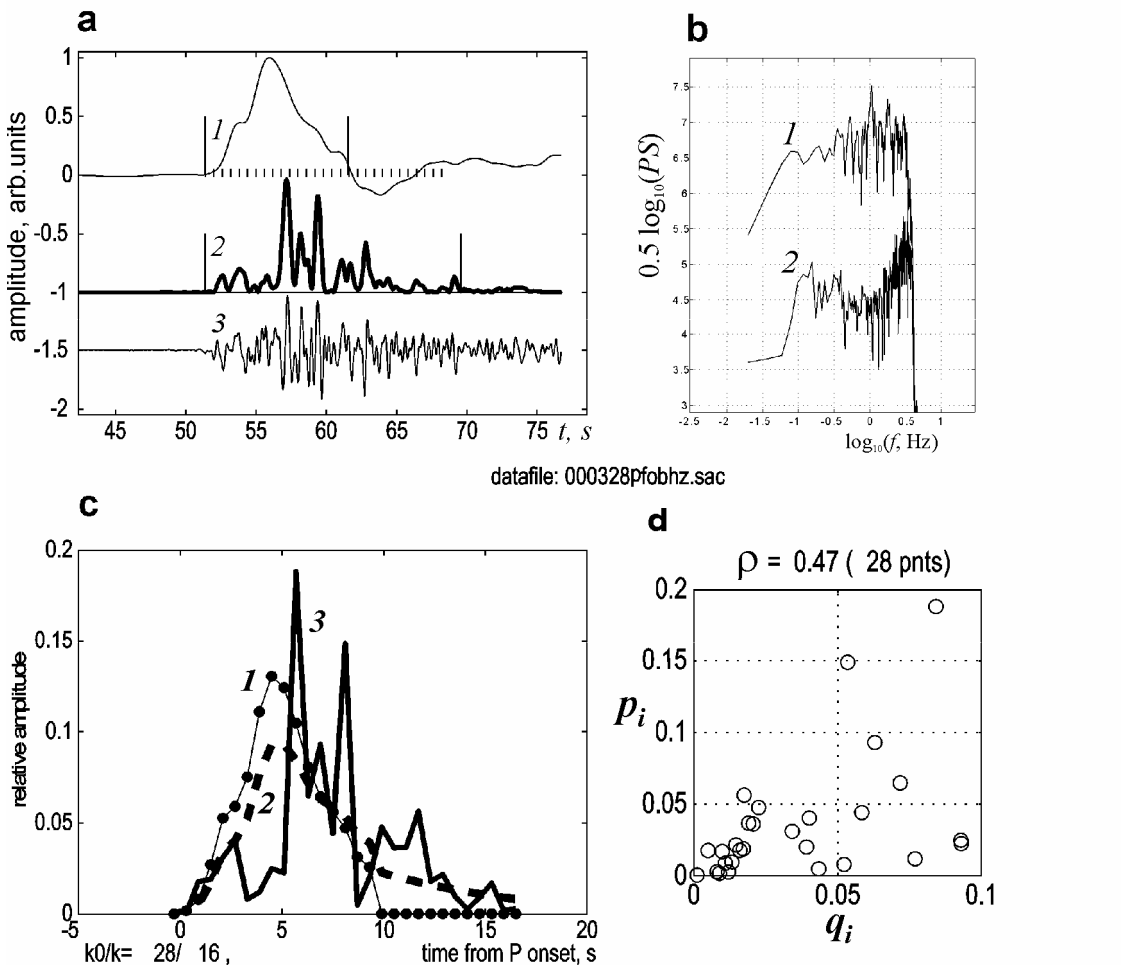

Figure 4. Processing procedure. a: displacement signal $m(t)$ (1), band-pass filtered velocity signal (3) and estimated power signal $p(t)$(2). b: control of the S/N ratio; (1): signal power spectrum (PS), (2): same for microseismic noise. Around 2.5 Hz, S/N becomes large. c: raw m_i (1) and modified q_i (3) displacement signal, and "power" signal p_i(3); d: correlation plot between q_i (abscissa) and p_i (ordinate).

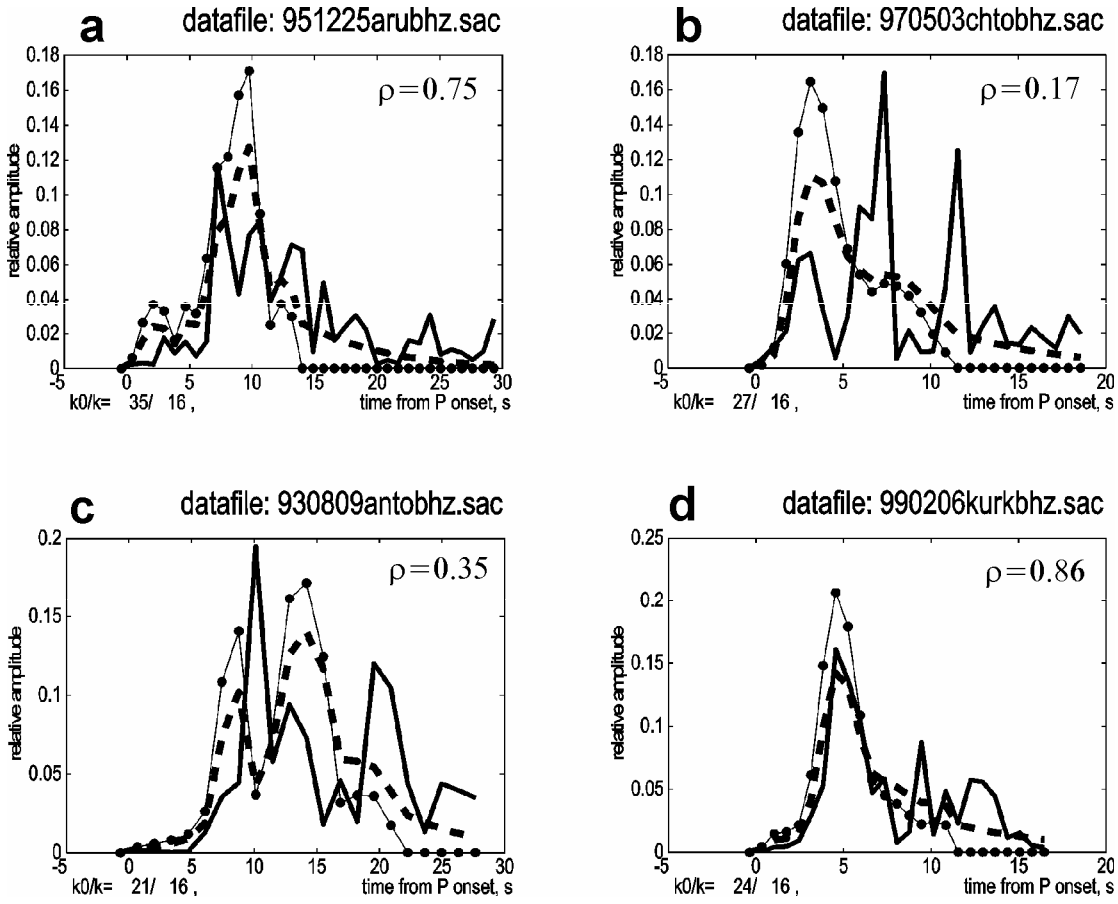

Figure 5. Examples of relatively good (a), exceedingly low (b), relatively low (c), and unusually good (d) correlation between p_i (HF power, solid line) and q_i (modified displacement, dashes) signals. Solid line: "power" signal, dots: "raw" displacement; dashes: modified displacement